

IV Assembly and Automation of the SPR Spectrometer

This chapter is dedicated to the description of the experimental set-up and the procedure used to perform SPR measurements. We start with a schematic picture of the optical system, followed by a description of the detectors fabricated in laboratory and a brief explication of the measurement procedures and software to collect and analyze the experimental data.

IV.1 Optical system

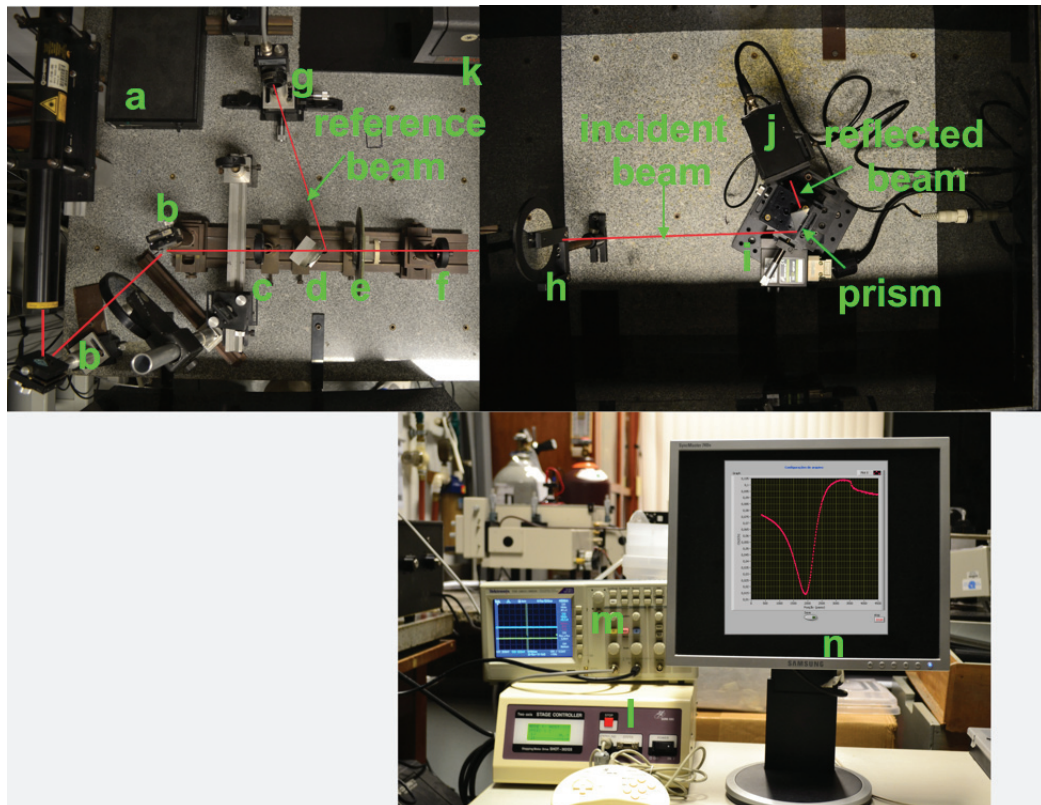


Figure IV.1: Photo of the automated SPR spectrometer: (a) laser source, (b) mirrors, (c,h) power attenuators, d-beam splitter, (e) linear polarizer, (f) pin-hole, (i) rotating stage, (g,j) detector, (k) black box, (m) oscilloscope, (n) PC.

The optical system assembled for SPR measurements in the Kreschmann configuration is shown in figure IV.1. A He-Ne laser (a) beam at the wavelength of 632.8 nm passes through power attenuators (c,h), a beam splitter (d), a linear polarizer (e) and a pin-hole (f) before impinging over the prism/sample system mounted over a motorized rotating stage (i) with a minimum angular step of 0.0025° (Sigma Koki, model SGSP-80Y AW, with controller Shot-202). The rotating base and the detector (j) used to measure the power of the beam reflected from the sample are kept inside a black box (k) of polypropylene, fabricated to isolate the system from external light and equipped with electrical connectors. The attenuators are used to avoid saturation of the detectors; the beam splitter is used to divide the exciting beam into a reference and an incident beam. The linear polarizer is aligned to create a TM-polarized incident beam, while the pin-hole is used to define a reference to measure the angle of incidence of the beam over the prism. The power of the reference beam is measured by a Silicon Photodiode (g) of ThorLabs (Model DET36A), while the signal reflected by the sample is measured by an home made large area Silicon Detector (j) which rotates together with the goniometer. The two signals are then sent to the input of a digital oscilloscope of Tektronic, model TDS1001c-30edu. The output signals of the oscilloscope and rotating motorized stages are finally sent to a personal computer and elaborated by an home-made software in LabView language which allows real-time monitoring of the SPR response.

IV.2 Home-made detector

The active element of the home-made detector is a Silicon photodiode characterized by a quite large area (1cmx2cm) to assure the detection of the signal reflected from the sample at high angle of incidence. The photodiode has a responsivity of 0.42 A/W at 632.8nm, and is linked to an amplifying stage in photovoltaic mode, generally used to measure DC signals of low intensity [Bur95]. The scheme of the electric circuit of the amplifier is shown in figure IV.2

The circuit basically consists in a current to voltage converter where the photodiode is directly connected to the inverting input of an integrated amplifier (model TL081). Because this circuit deals with low input signal, high resistance and high gain, it may oscillates unintentionally. Therefore, a small amount of capacitance C_1 is used to stabilize the signal. The gain of the amplifying stage is defined by the resistance R_1 , while R_3 controls the offset of the operational amplifier. The components R_2 and C_2 are a low pass filter, with a cutoff frequency of $f = 1/2\pi R_2 C_2 = 95$ Hz. The filter reduces the noise

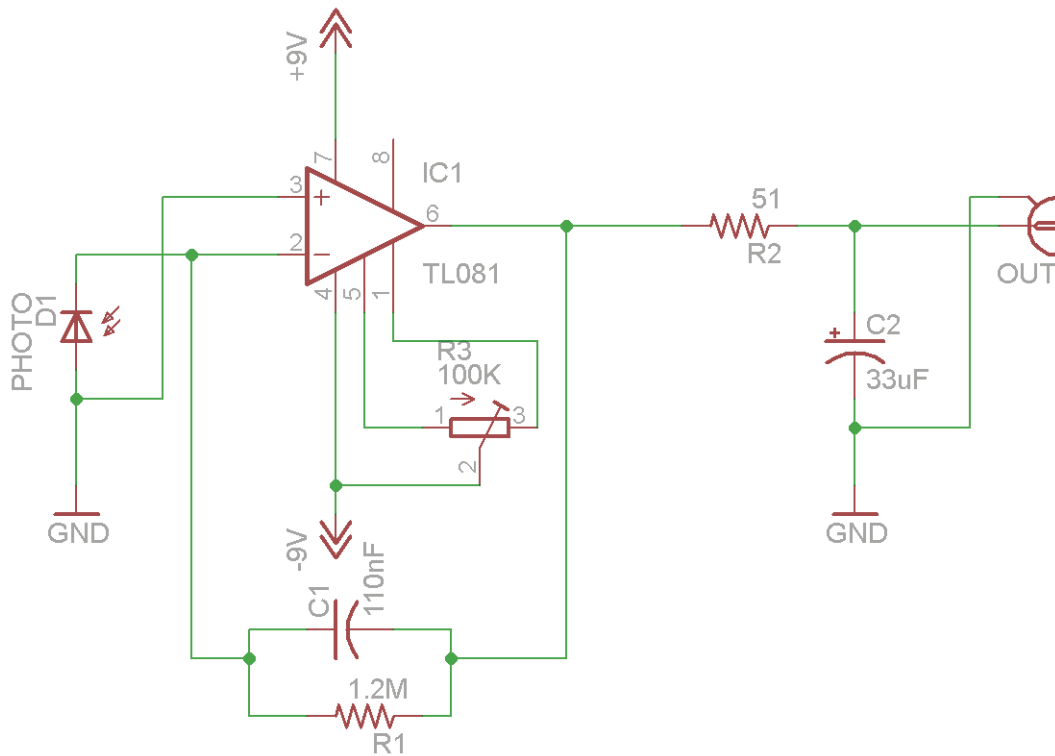


Figure IV.2: Electronic Scheme for of the silicon home-made detector.

in the output signal. In this configuration the gain of the detector is $-1.2 \text{ M}\Omega$. The home-made detector presents a linear behavior up to a response of 0.6 V . Figure IV.3 is a photo of the home-made detector.



Figure IV.3: Photo of the large area home-made detector.

IV.3 Definition of internal reflectivity and angle of incidence

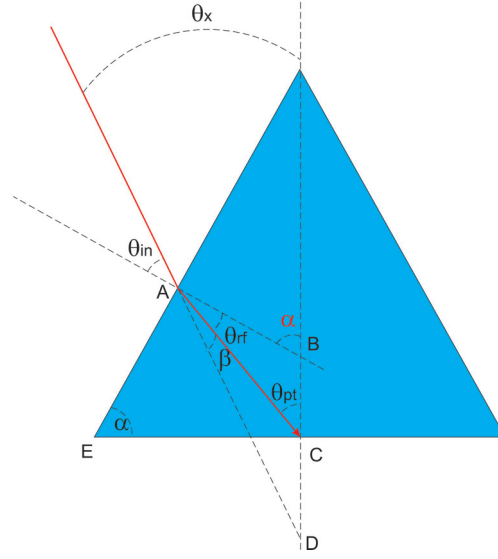


Figure IV.4: Scheme of the typical isosceles prism used for SPR coupling, θ_{in} is the angle of incidence that we measure directly with the goniometer, and θ_x is the angle of incidence related with θ_{in} , used by the elaboration data program (*Winspall* free software).

The picture IV.4 shows a generic isosceles prism with angle of base α as the ones used in our measurements. The angle of incidence that can be measured directly is the angle called θ_{in} , formed by the beam impinging on the external surface of the prism and the line perpendicular to this interface. When the rotating platform is moved from this position, the angle θ_{in} changes accordingly to the relation $\theta_{in} = 0.0025^\circ \times N_s$, where N_s is the number of steps counted by the goniometer to move from the 0-position to this angle. It is straightforward to demonstrate that the relations existing between the angles α , θ_{in} , θ_x , θ_{pt} as defined in figure IV.4 are the followings (See Appendix A):

$$\theta_x = \alpha - \theta_{in}, \quad (1)$$

$$\alpha = \arcsin \frac{1}{n_p} + \arcsin \frac{1}{n_p} \sin \theta_{in}, \quad (2)$$

$$\theta_{pt} = \alpha - \arcsin \left(\frac{1}{n_p} \sin (\alpha - \theta_x) \right), \quad (3)$$

$$\theta_x = \alpha - \arcsin (n_p \sin (\alpha - \theta_{pt})), \quad (4)$$

where n_p is the refractive index of prism. The software we used for the analysis of the experimental data consider θ_x as the angle of incidence and defines the

reflectivity R as the ratio of the power of the light reflected inside the prism by its hypotenuse and the power of the light impinging on the same face. Note that in our experimental set-up the detectors measure the power of the incident and reflected beams outside the prism. The reflection of the beam when passing the legs of the isosceles prism is taken into account by an angle-dependent correction factor [Rueda09] $C(\theta_x)$ that we apply to the measured reflectivity. It holds the relation

$$R_A(\theta_x) = C(\theta_x)R_M(\theta_x), \quad (5)$$

where R_A is the actual (internal) reflectivity and R_M the measured one. The correction factor is obtained from the Fresnel formulas [Pochi88][Jenkins01][Mencuccini95] and is defined as

$$C(\theta_x) = \frac{\sin^4(\theta_{ref} + (\alpha - \theta_x)) \cos^4(\theta_{ref} - (\alpha - \theta_x))}{\sin^2(2(\alpha - \theta_x)) \sin^2(2\theta_{ref})} \quad (6)$$

with

$$\theta_{ref} = \arcsin\left(\frac{1}{n_p} \sin(\alpha - \theta_x)\right). \quad (7)$$

IV.4 Measurement procedure and software for data collection

Each measurement starts with the manual search of the angle of reference $\theta_{in} = 0$. This condition is satisfied when the incident beam is reflected by the external surface of the prism exactly in the center of the pin-hole in front of the black box of figure IV.1 . We verified experimentally that this situation can be reproduced with a precision of 10 minimum steps of the motorized stage, corresponding to an angle of 0.0025° . In this condition the number of steps (N_s) counted by the goniometer are reset to 0 and the collection data software that we developed in LabView programming language is turned on. Using the collecting data software is possible to choose the initial and final positions of the scanning together with its angular step, and visualize on real-time the profile of the internal reflectivity R_A in function of the angle of incidence θ_x . Figure IV.5 is a typical image of the control panel of the software at the end of one measurement. The arrow on the image of the graph of R_M vs N_s is pointing the position of the reflectivity in correspondence of the critical angle of the glass/air interface. The exact position of the critical angle depends on the index of refraction of the prism and the angle of its base α . To perform our

SPR measurements we used a prism made of BAK1, a well known material with index of refraction equal to 1,574 at a wavelength of 632.8 nm, and base angle with a nominal value of 45° . The exact value of the prism angle may change between different independent measurements because of the contribution due to the thin film of glycerin that is put between the prism and the glass substrate to avoid multi-reflections effects. To take in account of this effect the home-made LabView software makes first a scanning of R_M vs N_s . The number N_s corresponding to the critical value is manually searched on the screen showing the measurement at the end of the scanning (figure IV.5). In the moment we wish to save the data, the PC asks you the value of N_s at critical angle. Once put this value, the computer automatically calculates the correspondent value of α and the values of θ_x . At this point the file with the values of R_A vs θ_x is created and saved.

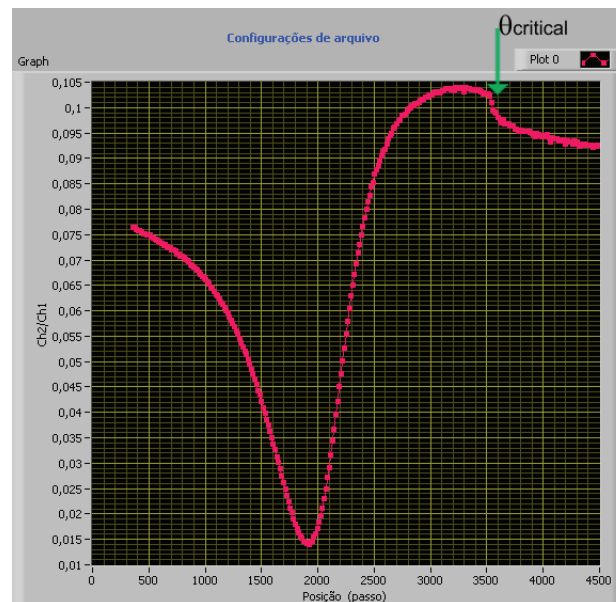


Figure IV.5: Typical curve of reflectivity R_M vs N_s , as shown on the control panel of the data acquisition software at the end of the measurement.

IV.5 Data elaboration software

The experimental data collected by our home-made LabView software are elaborated using the free software *Winspall* 3.02 available on line at the web page <http://www.mpip-mainz.mpg.de/knoll/soft/>. This software, elaborated by the group of Prof. Knoll at the Max Planck Institute for Polymer Research, computes the reflectivity of optical multilayer systems using the Fresnel equations and the matrix formalism. The inputs data sent to the program are the experimental data of the reflectivity R_A in function of θ_x together with an initial guess of the values of thickness and complex refractive index that

characterize each layer of the sample under analysis. The software starts then an iterative simulation trying to find the parameters of each layer that minimize the χ^2 (the difference between the experimental data and the simulation data) between the experimental and theoretical curves of R_A in function of θ_x . Figure IV.6 represents a typical image of the screen of the elaboration data software after a fit procedure on a fabricated sample with a thin film of silver of about 50 nm. The points represent the experimental data, the continue red line is the theoretical curve that minimize the χ^2 . The table is a list of the values of the index of refraction and thickness of each layer as computed by the program.

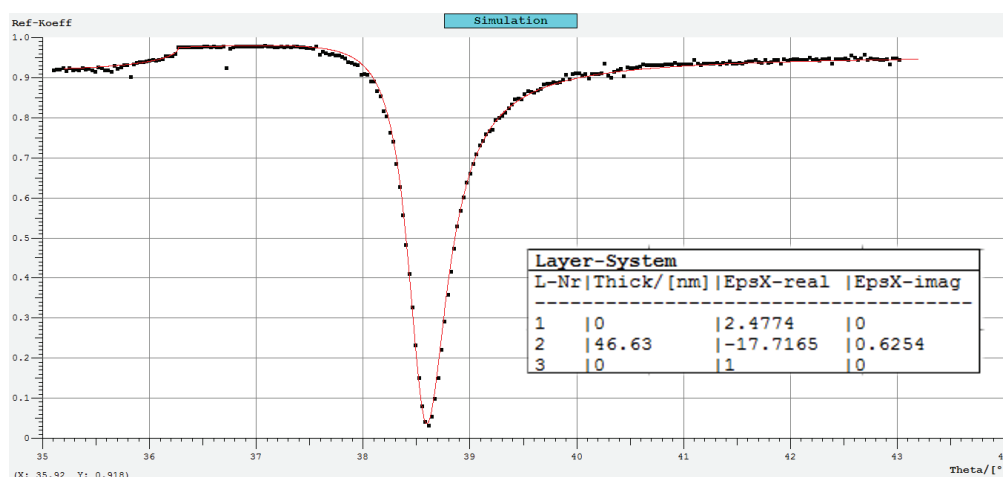


Figure IV.6: Experimental data for a silver film fitted using *Winspall*.